

# Constraining the equation of state of dense nuclear matter using thermal emission of neutron stars

**Nicolas Baillot d'Étivaux, Jérôme Margueron**

Univ Lyon, Université Claude Bernard Lyon 1, CNRS/IN2P3, Institut de Physique Nucléaire de Lyon, F-69622 Villeurbanne, France

**Sebastien Guillot, Natalie Webb**

CNRS, IRAP, 9 avenue du Colonel Roche, BP 44346, F-31028 Toulouse Cedex 4, France

**Márcio Catelan, Andreas Reisenegger**

Instituto de Astrofísica, Facultad de Física, Pontificia Universidad Católica de Chile, Av. Vicuña Mackenna 4860, 7820436 Macul, Santiago, Chile

**Abstract.** In this work, the equation of state (EoS) of the dense matter in the core of neutron stars (NSs) is based on a recently proposed meta-modeling of nuclear matter composed of nucleons, which can be parametrized by empirical quantities such as the energy density at saturation density or the nuclear incompressibility modulus. We use a set of recent observations of the thermal emission of seven NSs in quiescent low-mass X-ray binaries (qLMXBs) in order to find some constraints on the parameters of the meta-model, and thus on the nuclear EoS. This is done in a Bayesian statistical framework using Markov Chain Monte Carlo (MCMC) methods, to perform a simultaneous analysis over the seven sources. For the first time, the theoretical modeling of the EoS is directly implemented in the data analysis. We obtain constraints on the slope of the symmetry energy,  $L_{\text{sym}} = 37.2_{-8.9}^{+9.2}$  MeV, and give the first estimation of its curvature,  $K_{\text{sym}} = -85_{-70}^{+82}$  MeV, and on the isoscalar skewness parameter,  $Q_{\text{sat}} = 318_{-366}^{+673}$  MeV. Radii of about 12 km are preferred with a good fit statistic, yielding a nuclear EoS that is consistent with observational data and recent gravitational waves signals from NSs coalescence.

## 1. Introduction

The equation of state (EoS – the relation between pressure and density) of dense matter remains a crucial issue in fundamental physics, which has driven a lot of progress in the last decades. The matter in neutron star (NS) cores can reach several times the nuclear saturation density  $\rho_{\text{sat}} \sim 2.4 \times 10^{14}$  g.cm<sup>3</sup>, making them a key probe of the EoS in the high-density regime, which is hardly accessible in terrestrial experiments. There exist several approaches to describe this regime, based on different degrees of freedom such as nucleons, hyperons, or quarks and gluons which may appear at high densities [1].

In the present work, we use a recently proposed meta-modeling of cold catalyzed nuclear matter for the description of the NS core, improving a previously used constant radius approximation [2, 3, 4], or piecewise polytropes representation [5, 6, 7]. In our approach, the matter is composed only of neutrons, protons, electrons, and muons, which is realistic for central

densities up to  $3\text{--}4 \rho_{\text{sat}}$ , neglecting the possibility of a phase transition. Densities larger than  $3\text{--}4 \rho_{\text{sat}}$ , however, are likely to occur in very massive stars of about  $2 M_{\odot}$ , which seems not to be the case of the sources studied in the present work (see section 4).

For a given EoS, the Mass-Radius (MR) relation for NSs can be obtained by solving the Tolman-Oppenheimer-Volkov (TOV) equations [8, 9], so that measurements of masses and radii can provide strong constraints on the EoS [10]. One of the most employed methods to determine NS masses and radii is the observation of the thermal emission of quiescent low mass X-ray binaries (qLMXBs) [11, 12] in the soft X-rays (0.2 – 10 keV). Realistic atmosphere models have been developed along the years [13, 14] and have been applied to an increasing number of sources [3, 15], allowing to constrain the MR relation, and thus the dense-matter EoS. We use this method in the present work.

The first section briefly introduces the meta-modeling of the EoS and its application to NSs. The second describes the spectral modeling of the thermal emission and the Bayesian simultaneous analysis of our 7 selected sources, in order to constrain the meta-EoS. The third section summarizes our main results, and the fourth presents our conclusions.

## 2. Modeling the dense matter in the core of neutron stars

This meta-model (denoted as ELFc in [16, 17]) consists in the Taylor expansion of the potential part  $v(n, \delta)$  of the total energy density per baryon  $e(n, \delta) = t(n, \delta) + v(n, \delta)$  around nuclear saturation density, where  $t(n, \delta)$  is the kinetic energy per baryon,  $n = n_n + n_p$  is the sum of the neutron density  $n_n$  and proton density  $n_p$ , and  $\delta = (n_n - n_p)/n$  is the isospin asymmetry parameter. The potential term can thus be expressed as a function of the density parameter  $x = (n - n_{\text{sat}})/3n_{\text{sat}}$  as

$$v(n, \delta) = \sum_{\alpha=0}^N (v_{\alpha}^{\text{is}} + \delta^2 v_{\alpha}^{\text{iv}}) \frac{x^{\alpha}}{\alpha!} u(x), \quad (1)$$

where the function  $u(x)$  ensures that  $v(n, \delta) \rightarrow 0$  for  $n \rightarrow 0$  for any order  $N$  (see [16]). The parameters  $v_{\alpha}^{\text{is/iv}}$  of the expansion stand for the isoscalar (is) and isovector (iv) contributions to the energy. These coefficients are closely related to nuclear observable properties, such as the symmetry energy or the incompressibility modulus at saturation density. Some of these are well constrained in experiments, for example the energy at saturation density  $E_{\text{sat}}$  and the incompressibility modulus  $K_{\text{sat}}$ , while others are difficult to constrain, e. g. the slope of the symmetry energy  $L_{\text{sym}}$ , and some are not accessible in nuclear physics experiments, such as the skewness  $Q_{\text{sat/sym}}$  and the kurtosis parameters  $Z_{\text{sat/sym}}$ . A review of their experimental determination can be found in [16] and in references therein. In general, the lower-order terms can be better constrained, while the higher-order ones have a major impact at high density and are therefore difficult to constrain.

We use this meta-EoS to describe the core of NSs as described in [17], imposing some constraints: i) positiveness of the symmetry energy; ii) causality; and iii) the observational constraint that the maximum predicted mass for NSs should reach at least  $1.9 M_{\odot}$  to be consistent with the  $2\sigma$  lower limits of the measurements for PSR J1614–2230,  $1.908 \pm 0.016 M_{\odot}$  [18, 19, 20], and PSR J0348+0432 [21],  $2.01 \pm 0.04 M_{\odot}$ . The EoS from  $n_{\text{sat}}$  to approximately  $3n_{\text{sat}}$  depends mostly on the slope of the symmetry energy  $L_{\text{sym}}$ , the isovector incompressibility modulus  $K_{\text{sym}}$ , and the isoscalar skewness  $Q_{\text{sat}}$ . Thus, we treat these as free parameters, while the others are fixed to their central values presented in [17]. We explore a large number of MR relations by varying these three parameters, in order to confront the meta-EoS with observational data and constrain their values.

### 3. Confronting the meta-model with thermal emission from NSs

We analyse X-ray data of thermal emission from 7 qLMXBs in the globular clusters (GCs) M13 (NGC 6205), M28 (NGC 6266), M30 (NGC 7099), NGC 6304, NGC 6397,  $\omega$  Cen (NGC 5139), and X-7 in 47 Tuc (NGC 104), coming from the *XMM-Newton* and *Chandra* observatories (using the *XSPEC* software and the related *PyXSPEC* package [22]) to constrain the empirical parameters of the meta-EoS as well as the emission model parameters. Details on the data reduction can be found in [23]. Thermal emission of NSs can be modeled with realistic atmosphere models [24, 13] allowing to estimate the red-shifted temperatures and radii of the sources, leading to an estimation of their real masses and radii. NSs in quiescence do not undergo outbursts and show nearly pure thermal emission from the inner layers, which crosses the atmosphere of the star and the interstellar medium (ISM) before reaching the detectors. It is reasonable to assume that the stars we have considered have a pure H atmosphere [25, 15, 26], so we use the *nsatmos* model [13], modulated by absorption of soft X-rays in the ISM using the *tbabs* model [27]. We also add a power law to account for possible non-thermal emission at higher energy and set the exponent of the power law to 1.5, leaving the normalization free in the fit (finding that this normalization is always consistent with 0). We also account for the pile-up for all *Chandra* spectra, even for low pile-up fraction, as suggested by [15], and include a multiplicative constant to account for absolute flux cross-calibration errors between *XMM-pn*, *XMM-MOS*, and *Chandra* detectors.

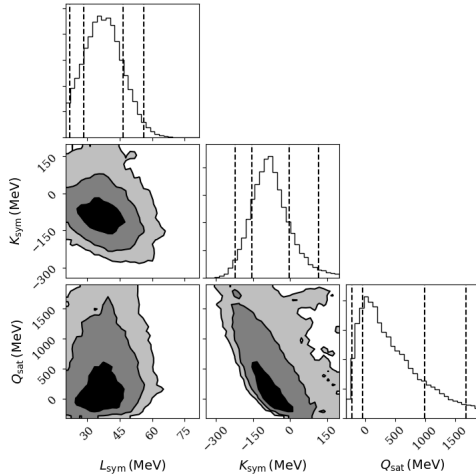
All the NSs in our analysis are assumed to be described by the same EoS and thus lie on the same MR relation. In the fit, their masses and radii are tied together by the parameterized EoS. The novelty of this approach is that the theoretical model is directly implemented in the analysis and the observational and theoretical parameters are treated on equal footing. With 7 sources, we end up with approximately 50 parameters, making MCMC methods appropriate. We use a *stretch-move* algorithm [28] with the python package *emcee* [29].

Since the distances are correlated with the radius [30] (the model being roughly a black body), we select sources in GCs because their distances can be accurately estimated [31]. The source distances are implemented within a Gaussian prior distribution considering the  $1\sigma$  estimation from [32], obtained from the individual  $X$ ,  $Y$ ,  $Z$  coordinate values, as shown in their Table C.3, using  $r_{\text{GC},\odot} = \sqrt{X^2 + Y^2 + Z^2}$ . Similarly, we include nuclear knowledge through a prior on the empirical parameter  $L_{\text{sym}}$ , which can be constrained in some experiments (see [33] for a detailed review), giving approximately  $L_{\text{sym}} = 50 \pm 10$  MeV. All the other observational parameters are sampled with a uniform distribution since we do not assume any constraints on them, as well as for the empirical parameters  $K_{\text{sym}} \in [-400; 200]$  MeV and  $Q_{\text{sat}} \in [-1300; 1900]$  MeV [17].

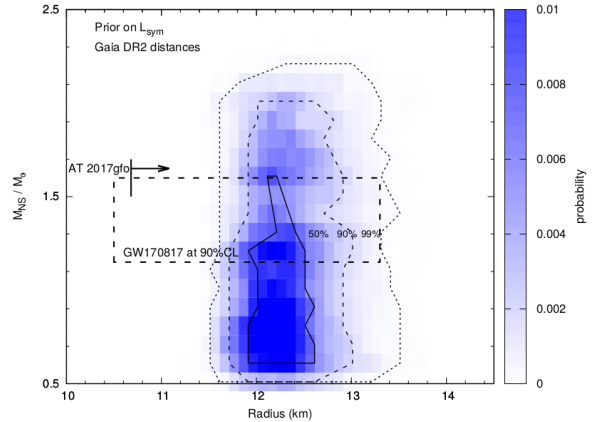
### 4. Results and comparison with recent works

Figure 1 illustrates the posterior probability distribution of the empirical parameters, while the posterior MR distributions for all the sources are shown in figure 2. The main result is that the posterior distributions of  $K_{\text{sym}}$  and  $Q_{\text{sat}}$  are rather well peaked in comparison with their initial uniform distribution, confirming that these parameters are well constraining the considered data. Note that the constraints we obtain,  $K_{\text{sym}} = -85^{+82}_{-70}$  MeV and  $Q_{\text{sat}} = 318^{+673}_{-366}$  MeV are the first estimations of these parameters coming from data, even with large uncertainties. The parameter  $L_{\text{sym}} = 37.2^{+9.2}_{-8.9}$  MeV is consistent with the prior imposed but lower values are preferred. This tension probably comes from the fact that the lower values of  $L_{\text{sym}}$  give lower radii at low masses, which seems to be favored for our sources as illustrated in figure 2, and giving  $R_{1.45} = 12.35 \pm 0.37$  km for a  $1.45 M_{\odot}$  NS, even if low masses are preferred in our analysis (see [23] for more details). We also find correlations among the empirical parameters, illustrating compensations between them, likely originating from the causality and stability requirements.

We also compare our contours in figure 2 with the constraints from AT2017gfo [34] and from GW170817 [35, 36, 37] and find that our results are consistent. A recent analysis in a similar framework [7] found  $R_{\text{NS}} = 11.2$ – $12.3$  km for a  $1.4 M_{\odot}$  NS and  $L_{\text{sym}} = 38.94$ – $58.09$  MeV,



**Figure 1.** Posterior probability distributions and correlations of the empirical parameters  $L_{\text{sym}}$ ,  $K_{\text{sym}}$  and  $Q_{\text{sat}}$ . On the two-dimensional correlation plots, the contours indicate the 1, 2, and  $3\sigma$  confidence areas while on the one dimensional posterior distributions, the dashed vertical line shows the 68% and 90% quantiles.



**Figure 2.** Mass-Radius posterior probability distributions considering all the 7 sources. The 50%, 90% and 99% confidence level are represented, as well as the constraints from AT2017gfo [34] and from GW170817 [35, 36, 37].

which is also consistent with our findings. Note that the main difference with our analysis is that we implemented the EoS directly in the fit instead of determining posterior distributions for masses and radii and then fitting to different EoSs. We also note that, in our case, the uncertainties are smaller. We also compare our results to other recent analyses using different methods [34, 38, 35, 36, 37] in [23].

## 5. Conclusions

We described NS cores with a recently proposed meta-modeling of nuclear matter [16, 17], disregarding the possibility of a strong first-order phase transition. The meta-model parameters having the strongest effect on the predicted MR relation of NSs are the slope of the symmetry energy  $L_{\text{sym}}$ , the isovector incompressibility  $K_{\text{sym}}$  and the isoscalar skewness  $Q_{\text{sat}}$ . By varying these parameters in a wide range, we sampled a large number of EoSs to confront the meta-model to observational data. We performed a simultaneous spectral analysis of the thermal emission of 7 qLMXBs in GCs, assuming a pure H atmosphere and accounting for pile-up, X-ray absorption in the ISM, and possible non-thermal emission. The novelty of our approach is the direct implementation of the EoS in the fit, treating observational and theoretical parameters on equal footing and avoiding over-constraints. Independent estimations of the distances to the sources [32] as well as for the slope of the symmetry energy  $L_{\text{sym}} = 50 \pm 10$  MeV [33] were taken into account through Bayesian priors. The robustness of our results concerning the priors, the number of free parameters or the sources considered in the fit are presented in detail in [23]. We obtained  $L_{\text{sym}} = 38 \pm 9$  MeV, as well as the first estimations of  $K_{\text{sym}} = -85.82^{+82}_{-70}$  MeV, and  $Q_{\text{sat}} = 318^{+673}_{-366}$  MeV from observational data. We also find an anti-correlation between  $K_{\text{sym}}$  and  $Q_{\text{sat}}$ , originating from the causality and stability constraints. We predict a radius  $R_{1.45} = 12.35 \pm 0.37$  km for a  $1.45 M_{\odot}$  NS, consistent with, but near the upper bounds, of other recent analyses [34, 38, 7, 35, 36, 37]. This is due to the inclusion of nuclear physics knowledge

through the EoS modeling in the fit.

The meta-model is currently being extended to a relativistic treatment of nucleons and the inclusion of a possible phase transition. The parameters of this new model will be constrained by the data in the same spirit as in the present work, including new observables such as those from the *Neutron Star Interior Composition ExploreR (NICER)* [39] and those coming from gravitational-wave signals obtained by the LIGO-Virgo collaboration.

## References

- [1] Oertel M, Hempel M, Klähn T and Typel S 2017 *Rev. Mod. Phys.* **89**(1) 015007
- [2] Guillot S, Servillat M, Webb N A and Rutledge R E 2013 *ApJ* **772** 7 (*Preprint* 1302.0023)
- [3] Guillot S and Rutledge R E 2014 *ApJL* **796** L3 (*Preprint* 1409.4306)
- [4] Guillot S 2016 *Mem. Soc. Astron. Italiana* **87** 521
- [5] Steiner A W, Lattimer J M and Brown E F 2013 *ApJL* **765** L5 (*Preprint* 1205.6871)
- [6] Öznel F, Psaltis D, Güver T, Baym G, Heinke C and Guillot S 2016 *ApJ* **820** 28 (*Preprint* 1505.05155)
- [7] Steiner A W, Heinke C O, Bogdanov S, Li C K, Ho W C G, Bahramian A and Han S 2018 *MNRAS* **476** 421–35
- [8] Tolman R C 1939 *Physical Review* **55** 364–73
- [9] Oppenheimer J R and Volkoff G M 1939 *Physical Review* **55** 374–81
- [10] Lattimer, J. M. and Prakash, M. 2007 *Phys. Rep.* **442** 109–65
- [11] Brown E F, Bildsten L and Rutledge R E 1998 *ApJL* **504** L95+ (*Preprint* arXiv:astro-ph/9807179)
- [12] Rutledge R E, Bildsten L, Brown E F, Pavlov G G and Zavlin V E 2002 *ApJ* **577** 346–58
- [13] Heinke C O, Rybicki G B, Narayan R and Grindlay J E 2006 *ApJ* **644** 1090–03
- [14] Haakonen C B, Turner M L, Tacik N A and Rutledge R E 2012 *ApJ* **749** 52
- [15] Bogdanov S, Heinke C O, Öznel F and Güver T 2016 *ApJ* **831** 184 (*Preprint* 1603.01630)
- [16] Margueron J, Hoffmann Casali R and Gulminelli F 2018 *Phys. Rev. C* **97** 025805
- [17] Margueron J, Hoffmann Casali R and Gulminelli F 2018 *Phys. Rev. C* **97** 025806
- [18] Demorest P B, Pennucci T, Ransom S M, Roberts M S E and Hessels J W T 2010 *Nat.* **467** 1081–83
- [19] Fonseca E 2016 *The Astrophysical Journal* **832** 167
- [20] Arzoumanian Z, et al. 2018 *The Astrophysical Journal Supplement Series* **235** 37
- [21] Antoniadis J, et al. 2013 *Science* **340** 448 (*Preprint* 1304.6875)
- [22] Arnaud K A 1996 XSPEC: The First Ten Years *Astronomical Data Analysis Software and Systems V (Astronomical Society of the Pacific Conference Series* vol 101) ed Jacoby G H and Barnes J p 17
- [23] Baillot d'Étivaux N, Guillot S, Margueron J, Webb N A, Catelan M and Reiseneger A 2019 *Preprint* arXiv:astro-ph/1905.01081
- [24] Zavlin V E, Pavlov G G and Shibanov Y A 1996 *A&A* **315** 141–152 (*Preprint* arXiv:astro-ph/9604072)
- [25] Edmonds P D, Heinke C O, Grindlay J E and Gilliland R L 2002 *ApJL* **564** L17–L20 (*Preprint* 0107.1620)
- [26] Haggard D, Cool A M, Anderson J, Edmonds P D, Callanan P J, Heinke C O, Grindlay J E and Bailyn C D 2004 *ApJ* **613** 512–16 (*Preprint* arXiv:astro-ph/0312657)
- [27] Wilms J, Allen A and McCray R 2000 *ApJ* **542** 914–24 (*Preprint* astro-ph/0008425)
- [28] Goodman J and Weare J 2010 *CAMCos* **5** 65–80
- [29] Foreman-Mackey D, Hogg D W, Lang D and Goodman J 2013 *PASP* **125** 306–12 (*Preprint* 1202.3665)
- [30] Rutledge R E, Bildsten L, Brown E F, Pavlov G G and Zavlin V E 1999 *ApJ* **514** 945–951 (*Preprint* 9807.0158)
- [31] Watkins L L, van de Ven G, den Brok M and van den Bosch R C E 2013 *M.N.R.A.S.* **436** 2598–15
- [32] Gaia Collaboration, et al. 2018 *ArXiv e-prints* (*Preprint* 1804.09381)
- [33] Lattimer J M and Lim Y 2013 *ApJ* **771** 51 (*Preprint* 1203.4286)
- [34] Bauswein A, Just O, Janka H T and Stergioulas N 2017 *ApJ* **850** L34 (*Preprint* 1710.06843)
- [35] Annala E, Gorda T, Kurkela A and Vuorinen A 2018 *Physical Review Letters* **120** 172703
- [36] Abbott B P, et al. 2018 *Phys. Rev. Lett.* **121** 161101 (*Preprint* 1805.11581)
- [37] Tews I, Margueron J and Reddy S 2018 *Phys. Rev. C* **98** 045804 (*Preprint* 1804.02783)
- [38] Nättilä J, Miller M C, Steiner A W, Kajava J J E, Suleimanov V F and Poutanen J 2017 *A&A* **608** A31
- [39] Gendreau K and Arzoumanian Z 2017 *Nature Astronomy* **1** 895